COBEM 2021 26th International Congress of Mechanical Engineering
November 22-26, 2021, Virtual Congress, Brazil
ABCM Associação Brasileira de Engenharia e Ciências Mecânicas

COB-2021-0367
Modeling and control of thermal management systems of batteries applied on vessel hybrid power systems

Gustavo Passeti Andrade da Silva
Bruno Souza Carmo
University of São Paulo - Av. Prof. Luciano Gualberto, 380 - Butantã, São Paulo - SP, 05508-010
gustavo.passeti@usp.br
bruno.carmo@usp.br

Abstract. *With the necessity of moving toward greener power systems, the International Maritime Organization set goals that are helping to pave a path to hybrid and even fully electric vessels. In that scenario, lithium-ion batteries emerge as an alternative solution for energy storage system and usually this kind of battery requires some sort of thermal management, specially under high power demand. A lot of works studied different techniques of thermal management. This paper develops two different models to compare which strategy is better efficiency wise. In both models, a cascade non-linear model predictive controller is used to control battery's core temperature to any desired set-point. Finally, for a created current input, it was found that the liquid cooling strategy spends more energy than the air cooling strategy.*

Keywords: *Battery Thermal Management Systems, Hybrid power systems, Marine vessels, Non-linear model predictive control.*

1. INTRODUCTION

Greenhouse gases emission has been a growing society concern for years now. Several agendas were created aiming at containing and reducing emissions for the next decades. Looking specifically at the maritime sector, a major emission contributor figuring among the top 10 emission countries if considered a country by itself (Crippa *et al.*, 2019), it is possible to see the International Maritime Organization (IMO) taking action and setting audacious goals for 2050. Probably the one that stands out the most is taking ships and vessels emissions to half or lower the levels from 2008 (IMO *et al.*, 2018).

Such goals come with technological challenges and developments. Hybridization is looking promising as a short to medium term solution toward these goals, it may also assist on development of zero emission technologies at smaller scales first. In the work of Geertsma *et al.* (2017), it is suggested that hybridization may lead to 10-35% emission reductions depending on the hybrid architecture used. As a matter of fact, most of these types of power train use an Energy Storage System (ESS) and typically Lithium-ion Battery (LIB) is the choice. This kind of battery provides great energy density when compared to other battery technologies and LIB technology has already reached commercialization stage (Van Schalkwijk and Scrosati, 2002).

Energy demand on any transportation task can be extremely high and in the case of electrical components that high demand is associated with heat generation and temperature increase through Joule effect. In the case of LIBs it can be extremely harmful, once it operates safely and efficiently in temperatures between 273K to 328K while charging or 273K to 313K while discharging (Lu *et al.*, 2013). Extremely low temperatures cause sluggish response from the battery (Shi *et al.*, 2012) and extremely high temperatures may cause thermal runaway, acceleration on the aging process and fire (Wu *et al.*, 2019). Because of all that, most LIB applications require some kind of Thermal Management System (TMS) associated with it.

Multiple techniques can be used on a TMS, three of the most common are air cooling, liquid cooling and Phase Change Material (PCM) cooling. Typically for marine application the technique used is either air cooling or liquid cooling, mostly because PCM cooling strategies may not be appropriate due to high heat generation load and long operation time (Khateeb *et al.*, 2004).

Battery thermal management systems have been the interest of study in many works and many different approaches were studied. Some works look for an arrangement of battery module that is capable of minimizing the temperature difference between cells. In Yang *et al.* (2015), an optimization approach was used to find the best arrangement for air cooling strategy. In Zhao *et al.* (2019), a tube with variable geometry that increases heat exchange area as liquid increases temperature was studied, with that the difference between the first and last battery of the pack could be diminished. More into controls and models, works like Lopez-Sanz *et al.* (2016) introduce the use of model predictive control in road vehicles to guarantee battery operation at an optimal temperature range and in Schimpe *et al.* (2018) a TMS on maritime

application was modelled.

This paper studies two TMS strategies, one air based and the other liquid based, both using a Non-linear Model Predictive Control (NMPC). All of that is presented in details in the following sections showing a general view of the systems, models used, controller and tuning proposed and finally results from simulations and discussions about which approach brings better energy efficiency for a thermal management system.

2. SYSTEM DESCRIPTION

Generally ESS, in marine application, are kept in containers and disposed in racks. Some manufacturers already have battery containers with a functional thermal management system in their catalogs (Fig. 1).

Figure 1. Example of container energy storage system from catalog.

For this study, due to the lack of information about the entire system, a system will be built based on information from Schimpe *et al.* (2018) and catalogs. Therefore, each module is built to have nominal energy of 600 Wh, made out of A26650 LIB (26 mm of diameter and 65 mm of height) in a 9Sx9P configuration. The container has size of a regular 20 ft container and is capable of storing up to 480 modules in a 4SX120P configuration, totalizing 288 kWh of nominal energy.

2.1 Air Cooling System

The first cooling systems modelled uses air as cooling fluid and consists in a HVAC controlling temperature inside a container and fans blowing air through the battery module. The battery module is assembled with $S_t = 35$ mm (transverse distance) and $S_l = 32$ mm (longitudinal distance) as Fig. 2 shows. This module design was chosen because it delivers better temperature uniformity throughout the module and optimal heat exchange, when compared to staggered configuration and different distances of aligned configuration (Yang *et al.*, 2015).

In this case, the container will be considered insulated, consequently it does not exchange heat with the outsides. The total number of fans necessary depends on the selected fan size. For a fan with 560 mm of diameter (a small size fan for marine application) it would be necessary 30 fans to cover all area with air flux, where each fan is capable of blowing air through 16 modules (equivalent to 8 drawers from a rack).

2.2 Liquid Cooling System

Typically a liquid cooling strategy involves the use of a cooling device, either a chiller or a radiator, and a pump. A cooling device is used for controlling inlet fluid temperature in the module and a pump is used to pump fluid into the system. A specificity of this kind of TMS is that two approaches can be used, a direct contact and an indirect contact one.

A direct contact liquid cooling is not commonly used because it requires special oils and can be extremely expensive (Wu *et al.*, 2019). Consequently, an indirect approach is used for this model. It is based on the geometry presented on Zhao *et al.* (2019), where aluminum cooling channels allow heat exchange between fluid and battery to happen. These channels have a unique geometry that enlarges contact area between tube and cell through variations of Θ, as Fig. 3 shows.

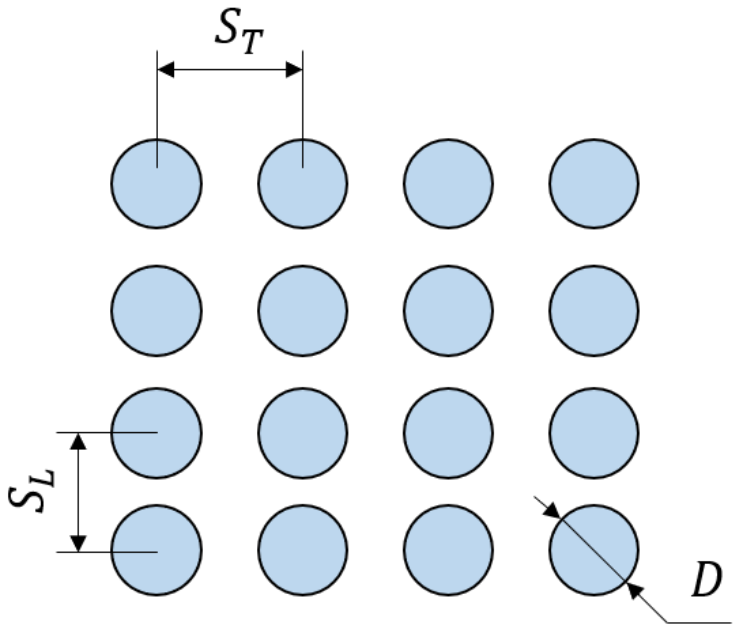

Figure 2. Schematic of battery module design for air cooling strategy.

Values of Θ typically vary up to 50.75°, thickness in the contact area is approximately 0.5 mm and channel's height and width are equal to 2 mm and 63 mm, respectively.

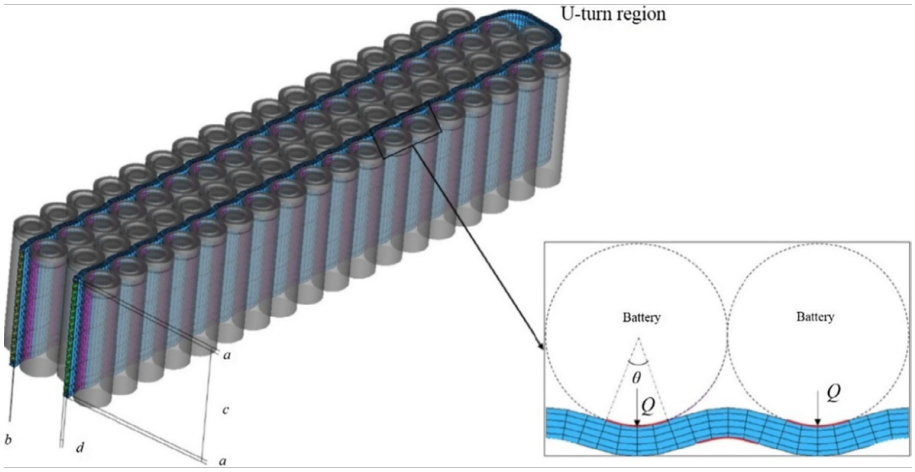

Figure 3. Schematic of battery module design for liquid cooling strategy (Zhao *et al.*, 2019).

Rounding everything up, the purposed system uses 30 pumps and chillers on an indirect channeled liquid cooling approach, the fluid used is a water/glycol mixture and the assumption of disregarding conduction heat transfer and heat losses is used.

3. COMPONENTS MODELS

3.1 Fan and Pump Models

The main objective on the fan/pump model is understand how volume flow correlates to power consumption in this kind of component. It is well known that this relations is close to a third order polynomial and a lot of parameters can affect this. However, for this model, a general approach that uses physical dimensions, fluid properties and an assumption of static fluid on the inlet will be used. With that, the relation can be described by:

$$P_{flux} = \frac{Q^3 \rho^2}{2 A_{flux}^2 \eta_{flux}} \tag{1}$$

where P_{flux} is the necessary power, A_{flux} stands for the outlet area of the equipment, ρ is the fluid density, η_{flux} is the

equipment's efficiency and Q is the volume flow rate. Physical parameters and characteristics of each equipment can be seen in Tab. 1.

Table 1. Parameters values for fan and pump models.

Parameters	**Fan**	**Pump**
P_{flux}, [W]	25 to 250	10 to 100
A_{flux}, [mm^2]	2462	128
ρ, [$\frac{kg}{m^3}$]	1.15	1069
η_{flux}, [%]	50	50

3.2 Battery Model

A complete battery model consists of 3 sub models that correlate at some point. The electrical sub model determines the terminal voltage of the batteries. The thermal sub model estimates the temperature in the core of a battery cell, once it is practically impossible to directly measure and it is usually the spot with highest temperature in a cell. Finally, the last sub model is the aging model, which is capable of predicting when a battery is reaching the end of its life.

3.2.1 Electrical Model

For the electrical sub model is used a equivalent circuit model with two RC pairs, like that shown in Fig. 4. This model is also known as Thevenin model and uses two RC pairs because shows good accuracy without compromising computational performance (Choi and Chang, 2020).

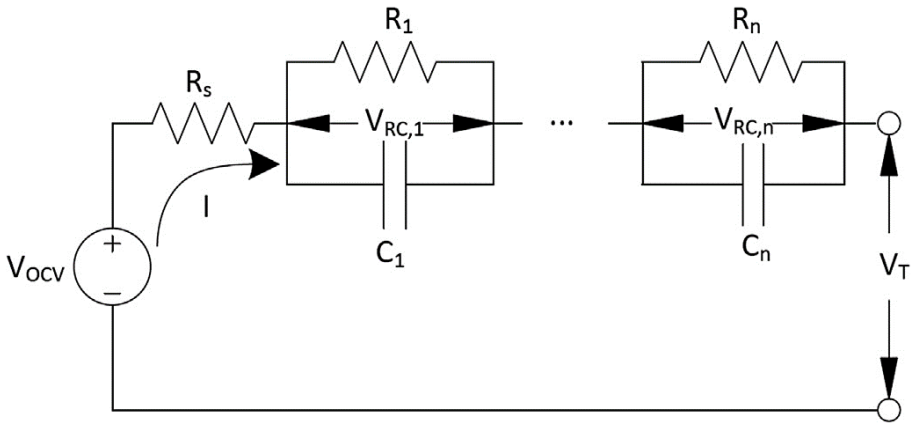

Figure 4. Equivalent circuit model representation (Lin *et al.*, 2014).

The parameters V_{OCV}, R_s, R_n and C_n of the model can be determined in bench tests and vary according to the state of charge (SOC), state of health (SOH) and battery temperature. For this model, the values used come from the work of Lin *et al.* (2014), in which the variation of these parameters was mapped under temperature and SOC variation.

Dynamic states described by this model are SOC,

$$\dot{SOC} = -\frac{I}{C_{bat}N_p}, \tag{2}$$

and tensions of both RC pairs,

$$\dot{V_n} = \frac{V_n}{R_nC_n} + \frac{I}{C_nN_p}. \tag{3}$$

From that, terminal voltage in the battery pack can be calculated via

$$V_{module} = N_s\left(V_{OCV} - V_1 - V_2 - R_s\frac{I}{N_p}\right), \tag{4}$$

where N_s is the equivalent number of battery cells in series, N_p is the equivalent number of battery cells in parallel and I is the current input on the energy storage container.

3.2.2 Thermal Model

Two states can be analyzed by the thermal model: surface temperature (T_s) and core temperature (T_c). The dynamics of each of these variables can be expressed based on energy balance and goes as it follows:

$$\dot{T}_c = \frac{Q_g}{C_c} + \frac{(T_s - T_c)}{R_c C_c} \tag{5}$$

$$\dot{T}_s = \frac{Q_f}{C_s} - \frac{(T_s - T_c)}{R_c C_s} \tag{6}$$

In the equations above, Q_g stands for the heat generated by a battery module and Q_f is the heat dissipated thought fluid flow. Generated heat can be calculated with an equation purposed by Bernardi *et al.* (1985). Nevertheless, there is a better approximation that does not bring instability to the model (Lin *et al.*, 2014).

$$Q_g = \frac{I}{N_p}\left(V_{OCV} - \frac{V_{module}}{N_s}\right) \tag{7}$$

Dissipated heat is calculated as stated below.

$$Q_f = hA_{cont}\left(T_{bi} - T_s\right) \tag{8}$$

Parameters like C_c, C_s and R_c are thermal capacity of battery's core, thermal capacity of battery's surface and equivalent thermal resistance of the battery respectively. Those values are determined in Lin *et al.* (2014).

In the dissipated heat equation there is a variable T_{bi} that stands for fluid inlet temperature. It has its own dynamics that will be better described in following sections. Still looking at Eq. (8) is worth mentioning that A_{cont} is the area of the battery cell that exchanges heat with the fluid and varies according to cooling strategy. Like contact area, heat transfer coefficient depends on the cooling strategy and can determined through Nusselt's empirical number correlation. For the air cooling approach the Zukauskas' Nusselt correlation is used

$$Nu_{air} = CRe_D^m Pr^{0.36}\left(\frac{Pr}{Pr_s}\right)^{0.25} \tag{9}$$

and for liquid cooling the Dittus-Boelter's Nusselt correlation is used

$$Nu_{liq} = 0.023 Re_D^{0.8} Pr^n. \tag{10}$$

These correlations use several parameters that vary according to flow conditions and sometimes with thermal conditions. All this information is described in detail by Kreith and Manglik (2016).

3.2.3 Aging Model

The aging model is derived from an empirical equation based on tests and assumes an end of life (EOL) at 20% loss on battery's capacity (Perez *et al.*, 2017). From this formulation, the dynamic of SOH can be stated as

$$\dot{SOH} = -\frac{|I|}{2C_{bat}N_p N_c} \tag{11}$$

From SOH's dynamic, N_c is the number of cycles completed until battery's EOL, this value can be calculated based on what is presented by Zhang *et al.* (2017).

3.3 HVAC and Chiller Models

There are multiple ways of modelling components like HVAC and chiller, the less complex is that presented in Cartagena *et al.* (2018). In this model, the component is modelled as a whole and is based on temperature difference imposed on heating and cooling coils. The formulation is shown in the following equations:

$$T_{ins} = \delta T_{bi} + (1 - \delta)T_{amb} + \Delta_h - \Delta_c \tag{12}$$

$$P_{cool} = K_f \dot{m}_{ins}^2 + \dot{m}_{ins} c_p \left(\frac{\Delta_h}{\eta_{cool}} + \frac{\Delta_c}{COP}\right) \tag{13}$$

where T_{ins} represents the temperature of the fluid leaving the component, $\dot{m}_{ins}$ is the mass o fluid being insufflated or reciculated, Δ_c is the temperature difference imposed to the cooling coil, Δ_h is the temperature difference imposed

to the heating coil, δ is the recirculation rate, T_{amb} stands for ambient temperature, P_{cool} is the required power, K_f is a coefficient of energy consumption, COP is the coefficient of performance of the machine and η_{cool} is the heating efficiency of the machine. With that, the dynamics of inlet and outlet temperatures of the battery pack (T_{bi} and T_{bo} respectively) can be written as:

$$\dot{T}_{bi} = \frac{\dot{m}_{ins} c_p (T_{ins} - T_{bi})}{C_{fluid}} + \frac{\dot{m}_{fluid} c_p (T_{bi} - T_{bo})}{C_{fluid}} \tag{14}$$

$$\dot{T}_{bo} = -\frac{Q_f}{C_{fluid}} + \frac{\dot{m}_{fluid} c_p (T_{bi} - T_{bo})}{C_{fluid}} \tag{15}$$

The differences between HVAC and Chiller models are the numerical values of $\dot{m}_{ins}$, δ, Δ_h and Δ_c. The values of these parameters for both models are given in Tab. 2. Also, there are slight differences in the values used to calculate the power used in the process, in this case, parameters K_f, COP and η_{cool} from Eq. (13). This differences are pointed out in Tab. 2 too. Parameters with "-" mean that they are not used, once in cases like the chiller, the power necessary to recirculate the fluid is already provided by the pump.

Table 2. Parameters values for HVAC and Chiller models.

Parameters	**HVAC**	**Chiller**
c_p, $[\frac{kJ}{kgK}]$	1013	3323
δ, [%]	80	0
K_f, $[\frac{Ws}{kg}]$	65	-
m_{ins}, $[\frac{kg}{s}]$	10	-
Δ_h, [K]	0 to 5	0 to 2.5
Δ_c, [K]	0 to 30	0 to 20
η_{cool}, [%]	90	90
COP	4	4

4. CONTROLLER

The entire system functionality is based on two controllers. The first one is used to determine P_{flux} and a desired inlet fluid temperature (T_f) that takes the battery's core temperature to the reference. The second one is used for T_{bi} tracking T_f through the actuation of HVAC or chiller, depending on the strategy used. A general view of the control strategy and system model interactions can be seen in Fig. 5.

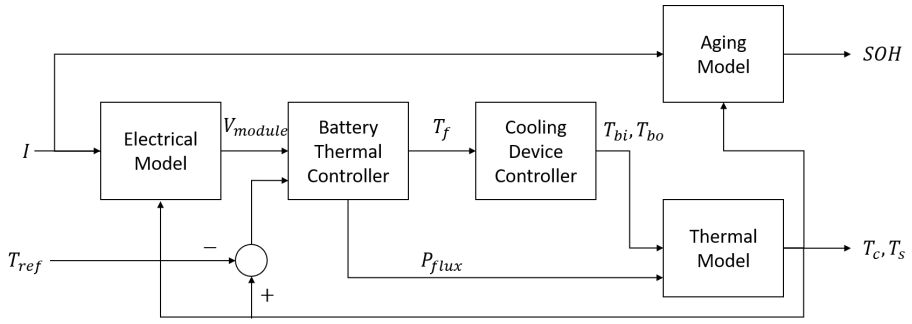

Figure 5. Block diagram representation of controller and system functionality.

The controller chosen is a non-linear model predictive control because it deals well with multiple control actions and all non-linearities of the system. NMPC also brings flexibility to the control allowing the use of different cost functions. For the purpose of this study, the cost function is defined as

$$J = \int_{t_0}^{t_f} \left(||x - x_{ref}||_Q^2 + ||u||_R^2 \right) \, dt \tag{16}$$

The tuning parameters in Eq. (16) are Q and R. Both are weighting matrices for states and controls respectively and are tuned according to Bryson's rule (Bryson and Ho, 2018). Therefore, for the thermal battery controller, states, controls and matrices are:

$$x = [T_c, T_s]^T; \qquad u = [P_{flux}, T_f]^T; \qquad Q = diag\left(\frac{1}{0.1^2}, 0\right); \qquad R = diag\left(\frac{1}{P_{fmax}^2}, \frac{1}{80^2}\right); \tag{17}$$

On the other hand, for the HVAC/Chiller, the controller parameters are:

$$x = [T_{bi}, T_{bo}]^T; \quad u = [\dot{m}_{ins}, \Delta_h, \Delta_c]^T; \quad Q = diag\left(\frac{1}{0.1^2}, 0\right); \quad R = diag\left(\frac{1}{m^2_{max}}, \frac{1}{\Delta^2_{hmax}}, \frac{1}{\Delta^2_{cmax}}\right); \tag{18}$$

Another important factor in the application of NMPC is the horizon prediction length (Nh). As the objective here is to reach a reference temperature and keep track of the inlet temperature the choices made were $Nh_{battery} = 30$ and $Nh_{cool} = 10$, so that both controllers would be able to track correctly with no significant stationary error.

5. METHODOLOGY

The entire code was written in MATLAB and used CasADi as an auxiliary tool to solve the non-linear optimization problem. CasADi is a powerful open source tool, that provides fast solution for non-linear programming problems (NLP) and can be easily implemented on other coding languages (Andersson *et al.*, 2019).

The integration method used is a fourth order Runge Kutta and due to a future application of this work, a time step of 0.1 s was used.

A synthetic current input was created to simulate both models (Fig. 6). In addition, three different reference values for core temperature were set along simulation in order to test the robustness of the controller.

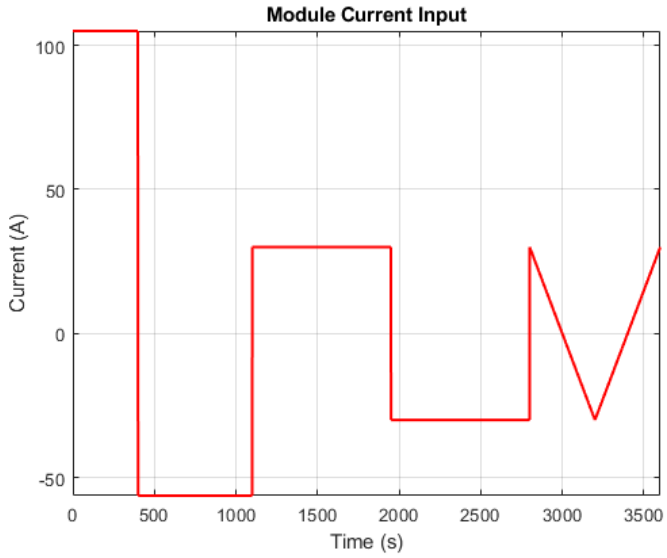

Figure 6. Synthetic current input for simulation.

6. RESULTS

Foremost, first thing to be done is to verify controller system's performance. Figure 7 shows that both TMS were capable of tracking reference temperature. However, liquid cooling strategy had a slower response and did not present relevant overshoot. This might represent the case of using less powerful components or weakening control tune on the air cooling system.

During the first 700s of simulation is possible to notice that core temperature does not go directly to 300K. It happens so, because of a sudden change in current input that happens at around 350s, at that point of time the battery goes from a fast discharge to a fast charge mode and due to a natural hysteresis that batteries have during that process a small instability in the model can be noticed.

In general both models responded well and were capable of going after the reference, therefore did not presented significant differences in core temperature values. Consequently, most of other results that can be provided by the model does not present relevant differences in value as Fig. 8 shows.

To compare the energy spent on each cooling system, actuation results were normalized for energy spent to control a single battery module instead of a entire container. Figure 9 compares the energy used to move the fluid on each system. There it is possible to see that most of the time the liquid cooling system requires less energy for the same task. Meanwhile, Fig. 10 compares the energy spent by the cooling device and is possible to notice that more power is required by the liquid cooling technique. That result was not expected at first but it makes sense once thermal inertia on the liquid cooling TMS is smaller, consequently chiller needs to actuate more to constantly keep tracking T_f.

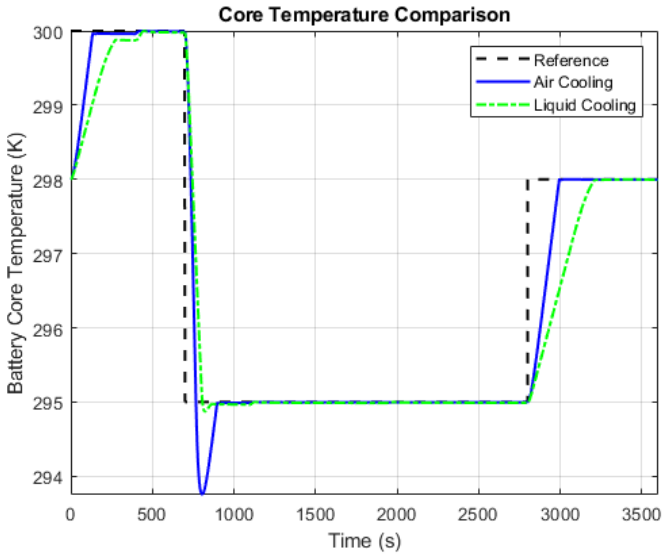

Figure 7. Comparison of core temperature results from air cooling and liquid cooling strategies.

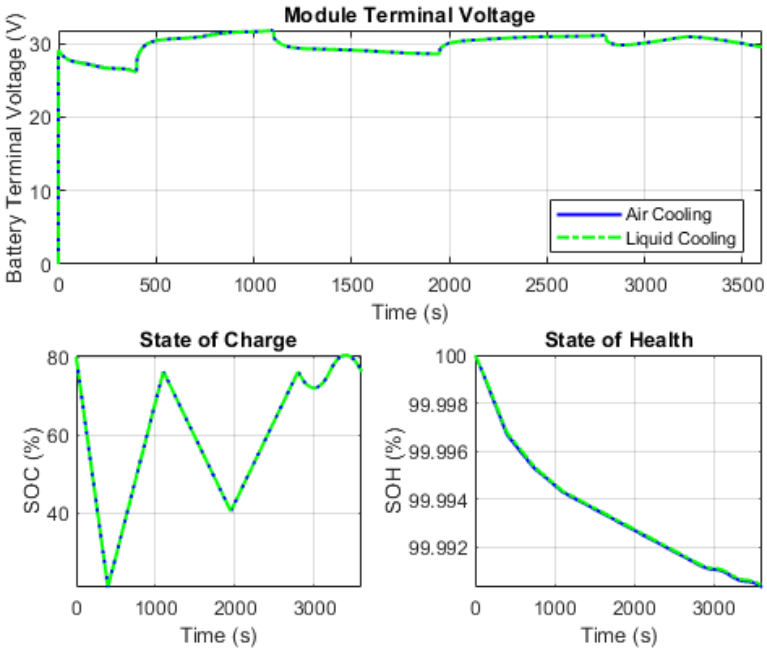

Figure 8. Three outputs from the model. On the upper it is presented the terminal voltage variation on the battery module. On the lower left the state of charge variation is presented and on the right side the state of health variation is presented.

In total, for this simulation, a liquid cooling strategy spends 72.24% more energy to accomplish the same task as an air cooling strategy. Such difference is considerably large and considering the fact of liquid cooling techniques being more expensive, it is hard to consider it a better option.

7. CONCLUSION

This paper successfully modelled two different thermal management systems for vessel application. Although, both need to be validated, they already provide qualitative results that allow comparisons between them to be drawn. As a result the liquid cooling system showed to be less energy efficient alongside a more complex and expensive system. However, it is not possible to infer that air cooling is better than liquid cooling. Many other designs need to be tested and in cases that it is necessary dealing with space issues, air cooling might not support the power demand.

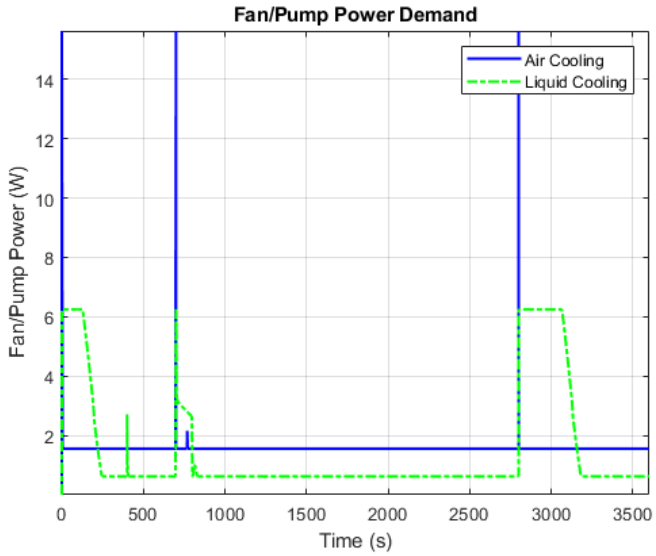

Figure 9. P_{flux} comparison between models.

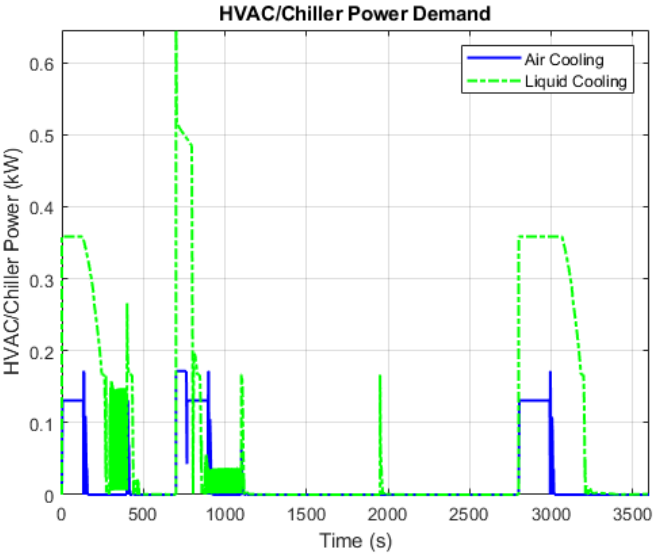

Figure 10. P_{cool} comparison between models.

8. ACKNOWLEDGEMENTS

We gratefully acknowledge support of the RCGI – Research Centre for Gas Innovation, hosted by the University of São Paulo (USP) and sponsored by FAPESP – São Paulo Research Foundation (2014/50279-4) and Shell Brasil, and the strategic importance of the support given by ANP (Brazil's National Oil, Natural Gas and Biofuels Agency) through the R&D levy regulation. B. S. Carmo thanks the Brazilian National Council for Scientific and Technological Development (CNPq) for financial support from in the form of a productivity grant, number 312951/2018-3. G. P. A. Silva thanks Coordination for the Improvement of Higher Education Personnel (CAPES) for the financial support from in the form of scholarship, number 33002010046P0.

9. REFERENCES

Andersson, J.A.E., Gillis, J., Horn, G., Rawlings, J.B. and Diehl, M., 2019. "CasADi – A software framework for nonlinear optimization and optimal control". *Mathematical Programming Computation*, Vol. 11, No. 1, pp. 1–36. doi:10.1007/s12532-018-0139-4.

Bernardi, D., Pawlikowski, E. and Newman, J., 1985. "A general energy balance for battery systems". *Journal of the electrochemical society*, Vol. 132, No. 1, p. 5.

Bryson, A.E. and Ho, Y.C., 2018. *Applied optimal control: optimization, estimation, and control*. Routledge.

Cartagena, O., Muñoz-Carpintero, D. and Sáez, D., 2018. "A robust predictive control strategy for building hvac systems based on interval fuzzy models". In *2018 IEEE International Conference on Fuzzy Systems (FUZZ-IEEE)*. IEEE, pp. 1–8.

Choi, E. and Chang, S., 2020. "A temperature-dependent state of charge estimation method including hysteresis for lithium-ion batteries in hybrid electric vehicles". *IEEE Access*, Vol. 8, pp. 129857–129868.

Crippa, M., Oreggioni, G., Guizzardi, D., Muntean, M., Schaaf, E., Lo Vullo, E., Solazzo, E., Monforti-Ferrario, F., Olivier, J.G. and Vignati, E., 2019. "Fossil co2 and ghg emissions of all world countries". *Luxemburg: Publication Office of the European Union*.

Geertsma, R., Negenborn, R., Visser, K. and Hopman, J., 2017. "Design and control of hybrid power and propulsion systems for smart ships: A review of developments". *Applied Energy*, Vol. 194, pp. 30–54.

IMO *et al.*, 2018. "Adoption of the initial imo strategy on reduction of ghg emissions from ships and existing imo activity related to reducing ghg emissions in the shipping sector". In *Note by the international maritime organization to the UNFCCC talanoa dialogue*, International Maritime Organization London, UK, pp. 1–27.

Khateeb, S.A., Farid, M.M., Selman, J.R. and Al-Hallaj, S., 2004. "Design and simulation of a lithium-ion battery with a phase change material thermal management system for an electric scooter". *Journal of Power Sources*, Vol. 128, No. 2, pp. 292–307.

Kreith, F. and Manglik, R.M., 2016. *Principles of heat transfer*. Cengage learning.

Lin, X., Perez, H.E., Mohan, S., Siegel, J.B., Stefanopoulou, A.G., Ding, Y. and Castanier, M.P., 2014. "A lumped-parameter electro-thermal model for cylindrical batteries". *Journal of Power Sources*, Vol. 257, pp. 1–11.

Lopez-Sanz, J., Ocampo-Martinez, C., Alvarez-Florez, J., Moreno-Eguilaz, M., Ruiz-Mansilla, R., Kalmus, J., Gräeber, M. and Lux, G., 2016. "Nonlinear model predictive control for thermal management in plug-in hybrid electric vehicles". *IEEE Transactions on Vehicular Technology*, Vol. 66, No. 5, pp. 3632–3644.

Lu, L., Han, X., Li, J., Hua, J. and Ouyang, M., 2013. "A review on the key issues for lithium-ion battery management in electric vehicles". *Journal of power sources*, Vol. 226, pp. 272–288.

Perez, H.E., Hu, X., Dey, S. and Moura, S.J., 2017. "Optimal charging of li-ion batteries with coupled electro-thermal-aging dynamics". *IEEE Transactions on Vehicular Technology*, Vol. 66, No. 9, pp. 7761–7770.

Schimpe, M., Naumann, M., Truong, N., Hesse, H.C., Santhanagopalan, S., Saxon, A. and Jossen, A., 2018. "Energy efficiency evaluation of a stationary lithium-ion battery container storage system via electro-thermal modeling and detailed component analysis". *Applied energy*, Vol. 210, pp. 211–229.

Shi, R., Xia, Q., Yang, J. and Ling, Z., 2012. "Low temperature performance analysis of li-ion batteries for electric vehicles". *Bus & Coach Technology and Research*, Vol. 2, p. 3.

Van Schalkwijk, W. and Scrosati, B., 2002. "Advances in lithium ion batteries introduction". In *Advances in Lithium-Ion Batteries*, Springer, pp. 1–5.

Wu, W., Wang, S., Wu, W., Chen, K., Hong, S. and Lai, Y., 2019. "A critical review of battery thermal performance and liquid based battery thermal management". *Energy conversion and management*, Vol. 182, pp. 262–281.

Yang, N., Zhang, X., Li, G. and Hua, D., 2015. "Assessment of the forced air-cooling performance for cylindrical lithium-ion battery packs: A comparative analysis between aligned and staggered cell arrangements". *Applied thermal engineering*, Vol. 80, pp. 55–65.

Zhang, D., Dey, S., Perez, H.E. and Moura, S.J., 2017. "Remaining useful life estimation of lithium-ion batteries based on thermal dynamics". In *2017 American Control Conference (ACC)*. IEEE, pp. 4042–4047.

Zhao, C., Sousa, A.C. and Jiang, F., 2019. "Minimization of thermal non-uniformity in lithium-ion battery pack cooled by channeled liquid flow". *International journal of heat and mass transfer*, Vol. 129, pp. 660–670.

10. RESPONSIBILITY NOTICE

The author(s) Gustavo Passeti Andrade da Silva and Bruno Souza Carmo are solely responsible for the printed material included in this paper.